Supporting Information

Synthesis and Protein Kinase C (PKC)-C1 Domain Binding Properties of Diacyltetrol Based Anionic Lipids

Narsimha Mamidi,‡ Subhankar Panda,‡ Rituparna Borah and Debasis Manna*

Department of Chemistry, Indian Institute of Technology Guwahati, Assam 781039, India.

Fax: (+) 91-361 258 2349; Tel: (+) 91-361 258 2325; E-mail: dmanna@iitg.ernet.in

Table of Content

Figure S1: Representative quenching plot of PKCδ-C1b fluorescence by ligand. Addition of increased concentration of DAT-PS_8 (0-58 μM) to PKCδ C1b (1 μM) quenched the intrinsic fluorescence intensity.

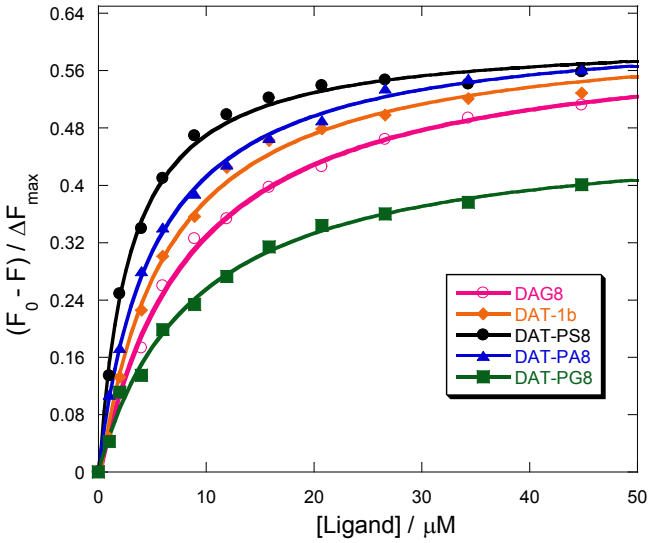

Figure S2: Binding isotherms of ligands with PKCδ-C1b. Representative plot of fluorescence intensity of PKCδ-C1b (1 μM) in buffer (20 mM Tris, 160 mM NaCl, 50 μM $ZnSO_4$, pH 7.4) in the presence of varying concentration of DAG_8, DAT-1b, DAT-PS_8, DAT-PA_8 and DAT-PG_8, where F and F_0 are fluorescence intensity in the presence and absence of the ligands, respectively. The solid lines are nonlinear least squares best fit curves.

Table S1. Anisotropy[a] values of the ligands in the presence and absence of the PKCδ, PKCθ and PKCα C1b/a proteins at room temperature.

Compound	PKCδ C1b	PKCθ C1b	PKCα C1a
buffer[b]	0.0746 (0.0007)	0.0682 (0.0222)	0.0522 (0.0071)
DAG_8[c]	0.2493 (0.0616)	0.3372 (0.0774)	0.1669 (0.0222)
DAT-**1b**[c]	0.3606 (0.0322)	0.3611 (0.0997)	0.4517 (0.0734)
DAT-PS_8[c]	0.4435 (0.0634)	0.4356 (0.0736)	0.3065 (0.0109)
DAT-PA_8[c]	0.2862 (0.0613)	0.4888 (0.0871)	0.3321 (0.0904)
DAT-PG_8[c]	0.3670 (0.0476)	0.3381 (0.1314)	0.2608 (0.0421)
DAG_{16}[c]	0.2737 (0.0630)	0.3993 (0.0814)	0.1958 (0.0188)
DAT-**1a**[c]	0.2953 (0.0786)	0.4413 (0.0758)	0.3802 (0.0165)
DAT-PS_{16}[c]	0.3509 (0.0761)	0.4525 (0.0914)	0.3417 (0.0075)
DAT-PA_{16}[c]	0.2828 (0.0694)	0.4713 (0.0631)	0.2843 (0.0887)
DAT-PG_{16}[c]	0.2773 (0.0304)	0.3282 (0.0620)	0.3542 (0.0571)
DAT-PS_{18}[c]	0.4341 (0.0126)	0.5147 (0.0357)	0.5730 (0.0166)
DAT-PA_{18}[c]	0.5664 (0.0368)	0.5038 (0.0648)	0.6770 (0.0469)
DAT-PG_{18}[c]	0.3856 (0.0475)	0.3827 (0.0821)	0.3841 (0.0407)

[a)] Values in parenthesis indicate standard deviations.
[b)] Protein, 1 μM in buffer (20 mM Tris, 160 mM NaCl, 50 μM $ZnSO_4$, pH 7.4).
[c)] Ligands, 10 μM; protein, 1 μM in buffer (20 mM Tris, 160 mM NaCl, 50 μM $ZnSO_4$, pH 7.4)

Figure S3: Representative protein-to-membrane FRET experiment under liposomal environment. Addition of increased concentration of compound DAG_8 (0 - 80 μM) to PKCδ C1b subdomain (1 μM) bound to the active liposome (PC/PE/dPE/DAT-PS_{16} (75/15/5/5)) decreases the FRET signal at 505 nm. All the measurements were performed in 20 mM Tris, pH 7.4 containing 160 mM NaCl and 50 μM $ZnSO_4$.

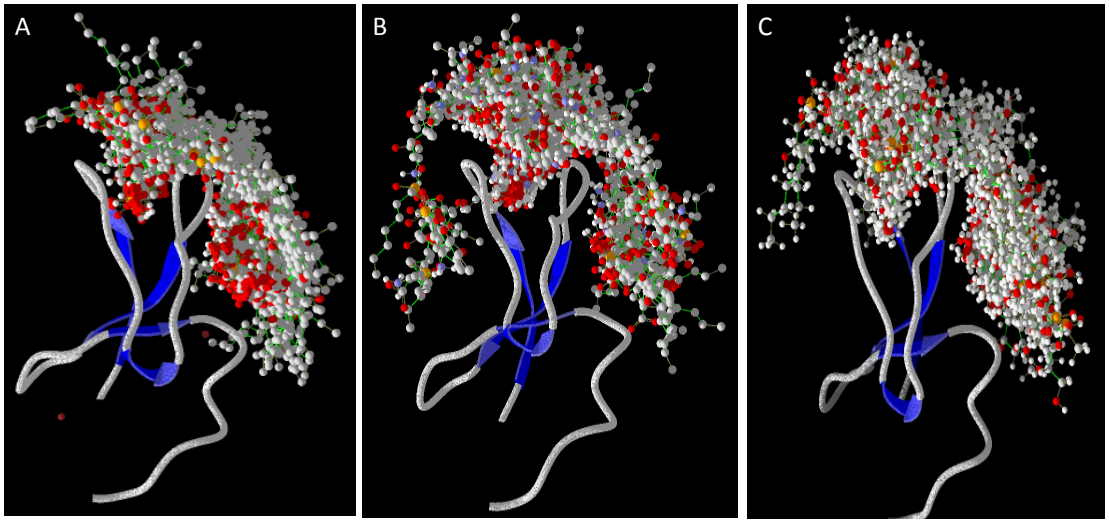

Figure S4: Structure of ligand bound PKCδ-C1b subdomain (PDB: 1PTR). (A) Modeled structures of DAT-PA_8 (A), DAT-PS_8 (B) and DAT-PG_8 (C) docked into PKCδ-C1b subdomain. The modeled structures were generated using Molegro Virtual Docker, version 4.3.0.

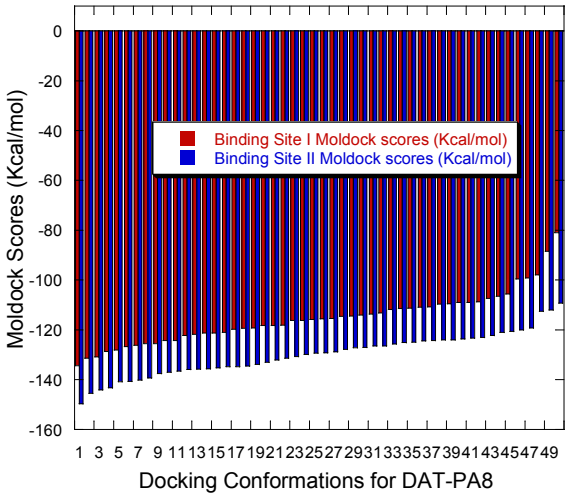

Figure S5: Theoretical binding energy calculation and distribution of DAT-PA_8 between the DAG/phorbol ester-binding site (I) and anionic lipid-binding site (II) of the PKCδ-C1b subdomain (1PTR).

^{1}H NMR and ^{13}C NMR Spectra of the New Compounds

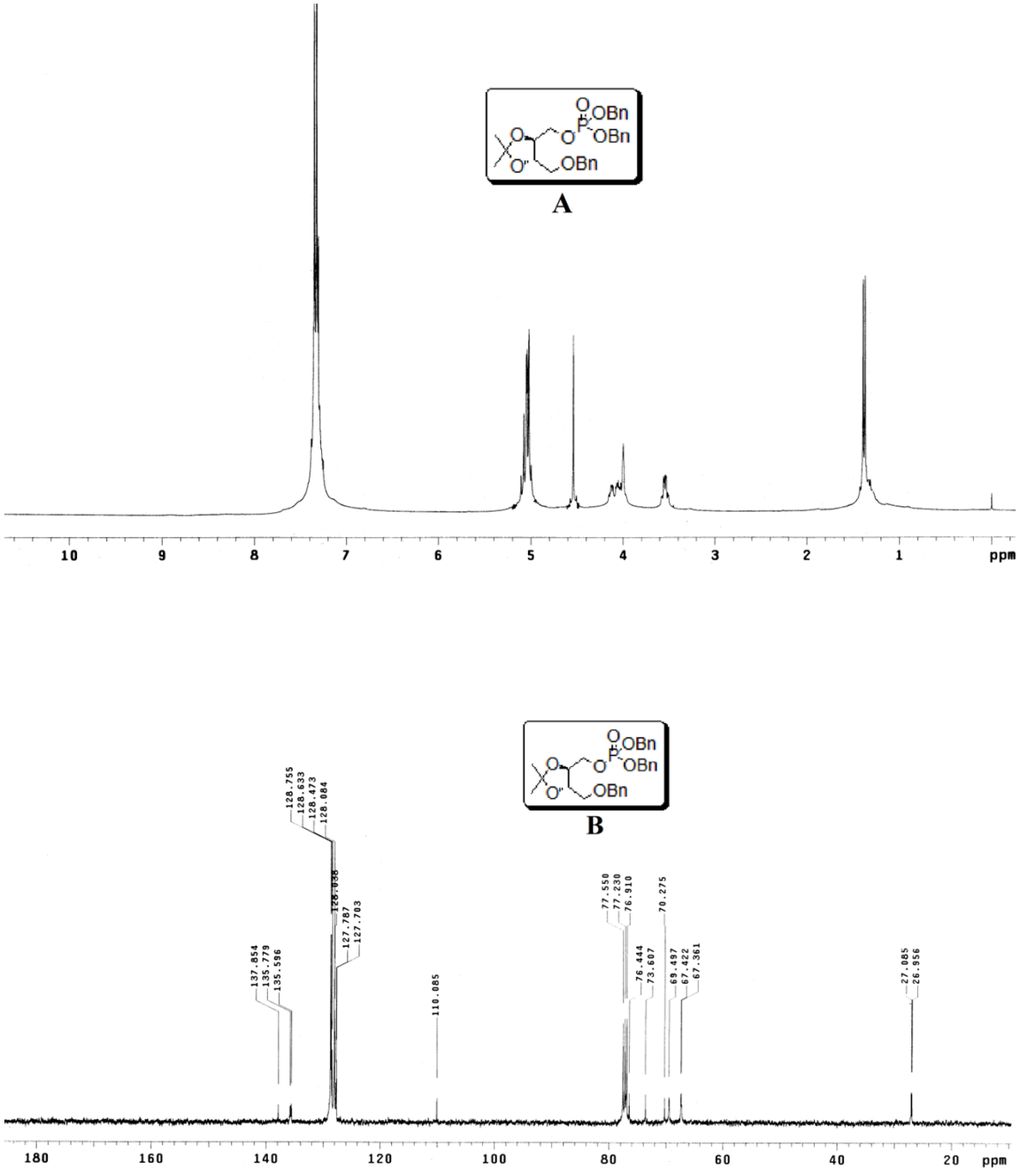

Figure S6. ^{1}H NMR (A) and ^{13}C NMR (B) spectra of compound **5**.

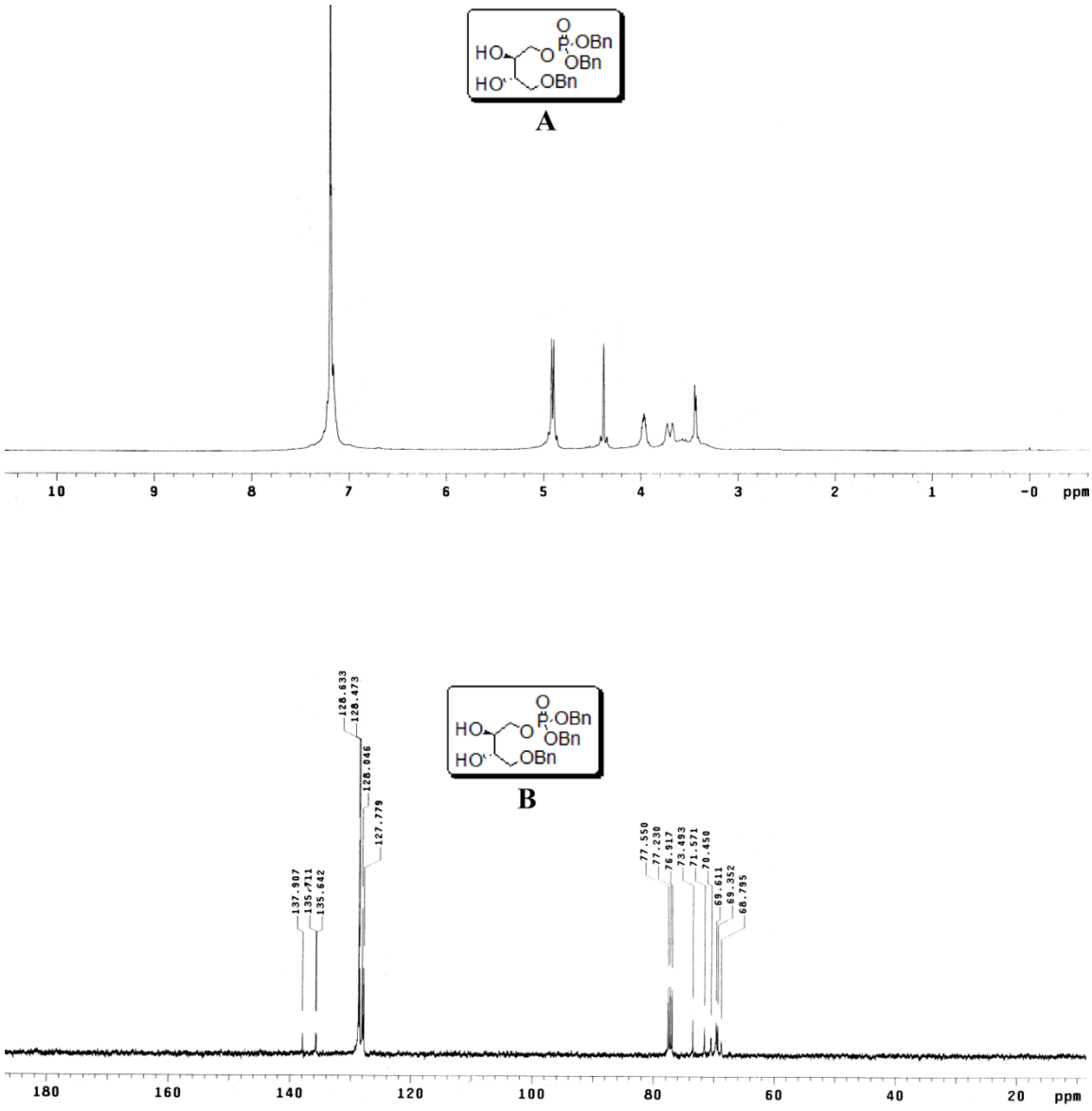

Figure S7. ^{1}H NMR (A) and ^{13}C NMR (B) spectra of compound **6**.

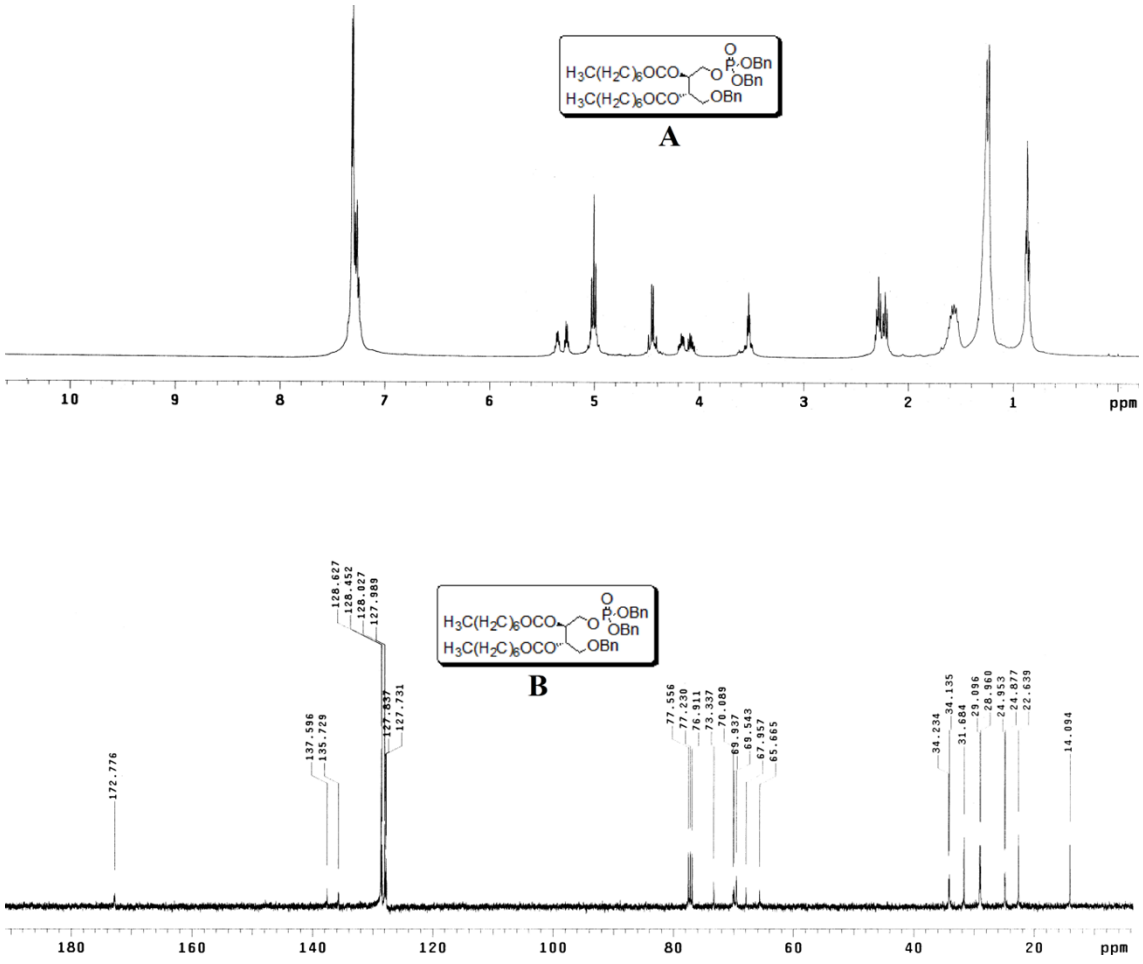

Figure S8. ^{1}H NMR (A) and ^{13}C NMR (B) spectra of compound **7**.

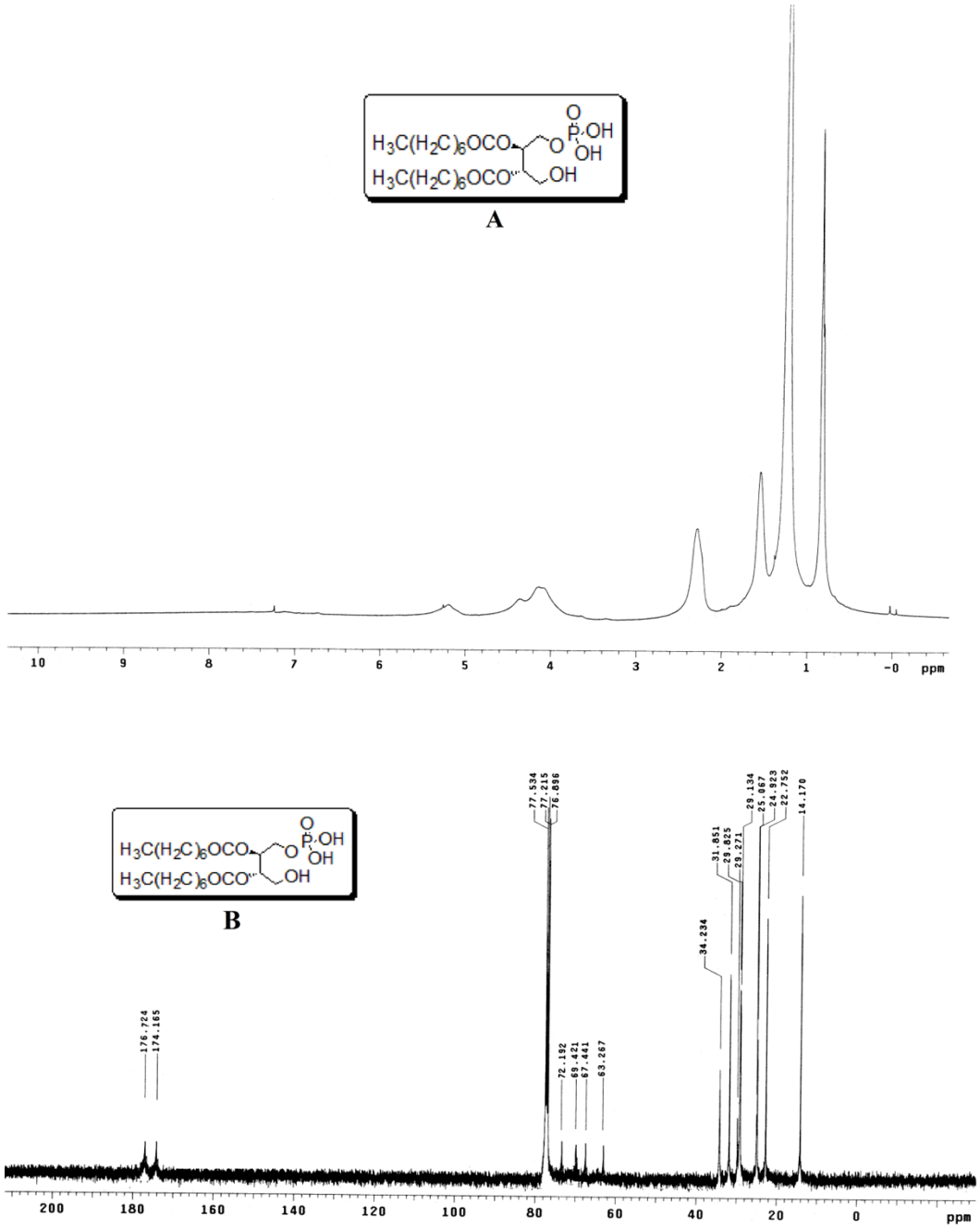

Figure S9. ^{1}H NMR (A) and ^{13}C NMR (B) spectra of DAT-PA_8.

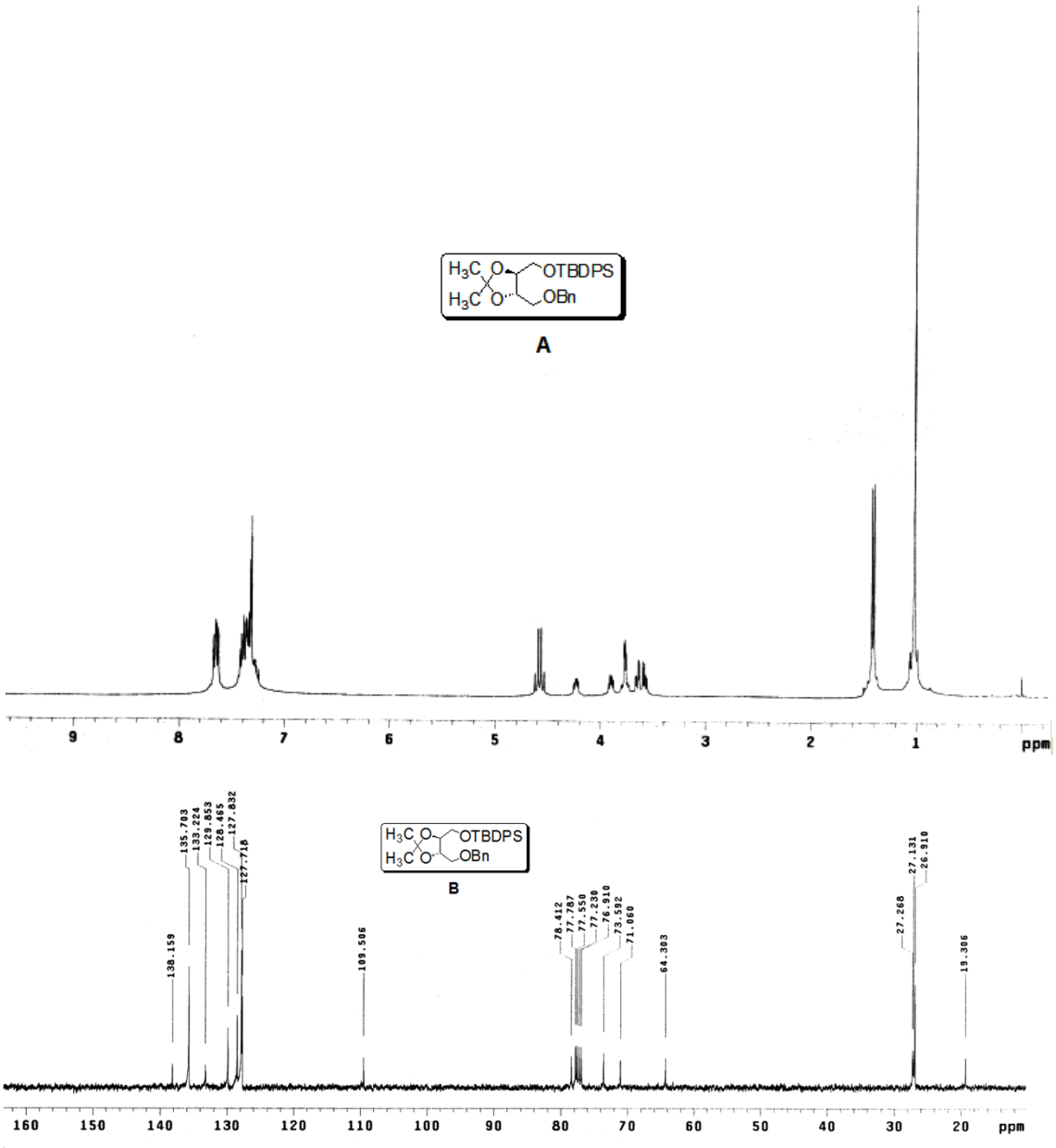

Figure S10. ^{1}H NMR (A) and ^{13}C NMR (B) spectra of compound **13**.

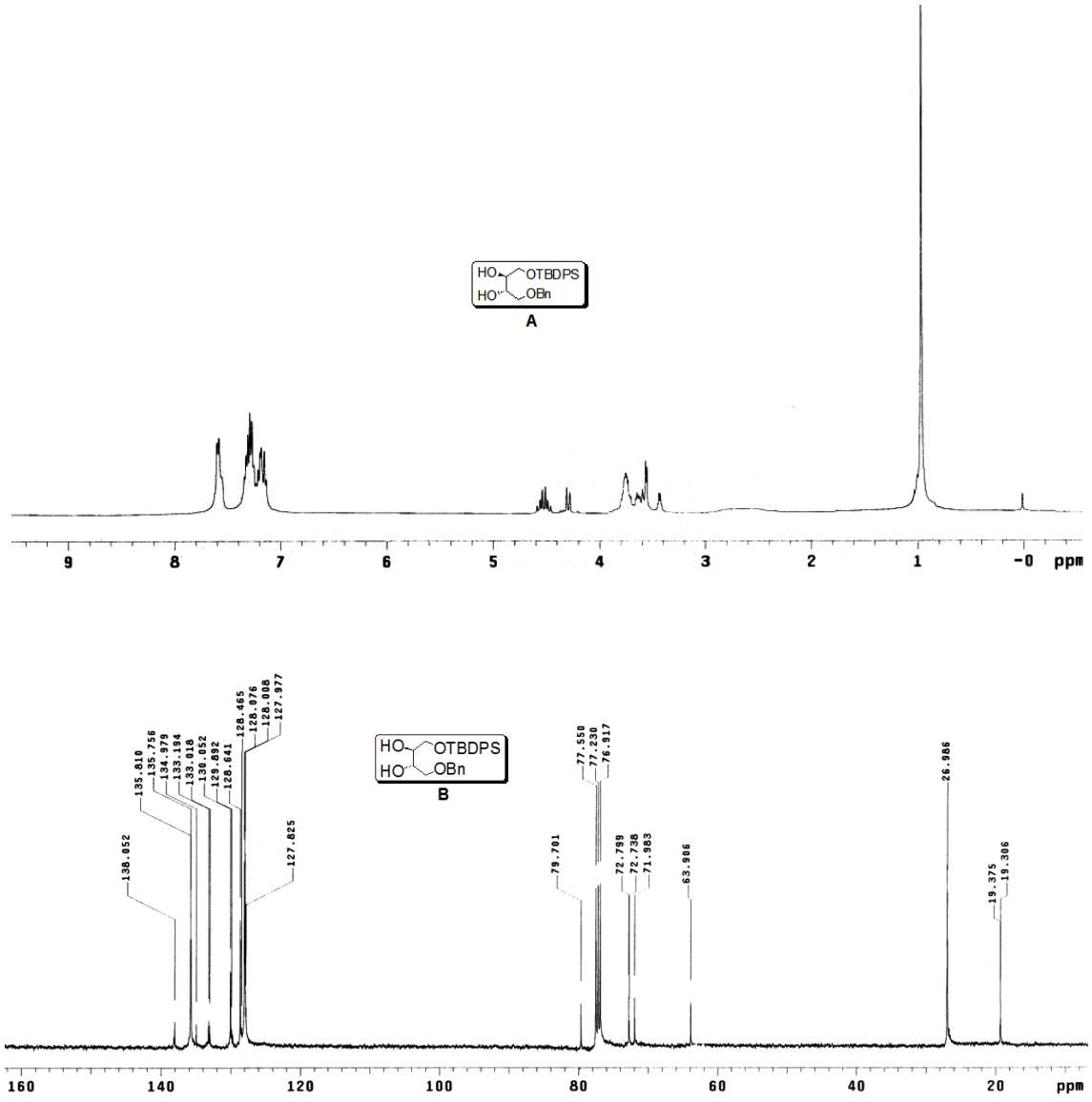

Figure S11. ^{1}H NMR (A) and ^{13}C NMR (B) spectra of compound **14**.

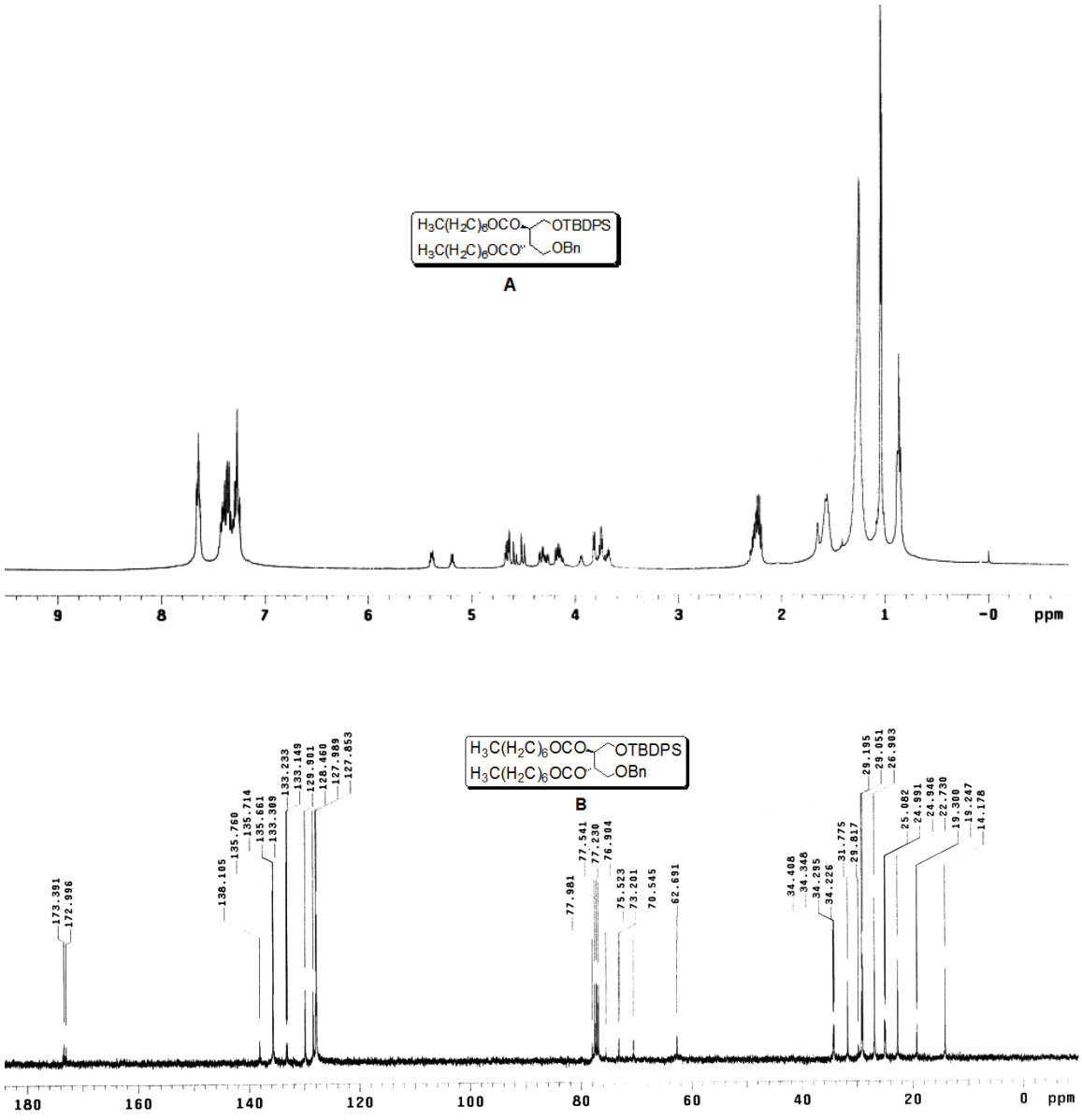

Figure S12. ^{1}H NMR (A) and ^{13}C NMR (B) spectra of compound **15**.

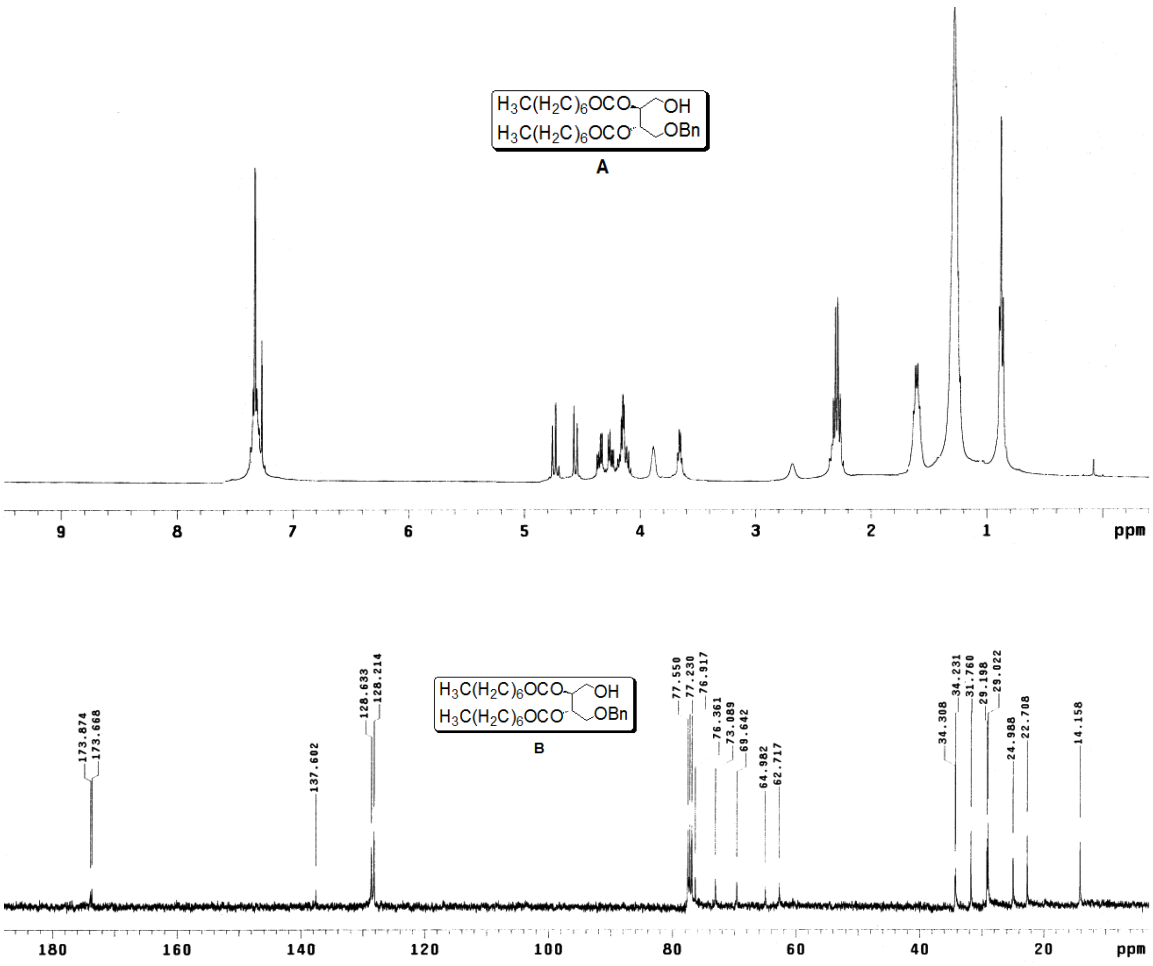

Figure S13. ^{1}H NMR (A) and ^{13}C NMR (B) spectra of compound **16**.

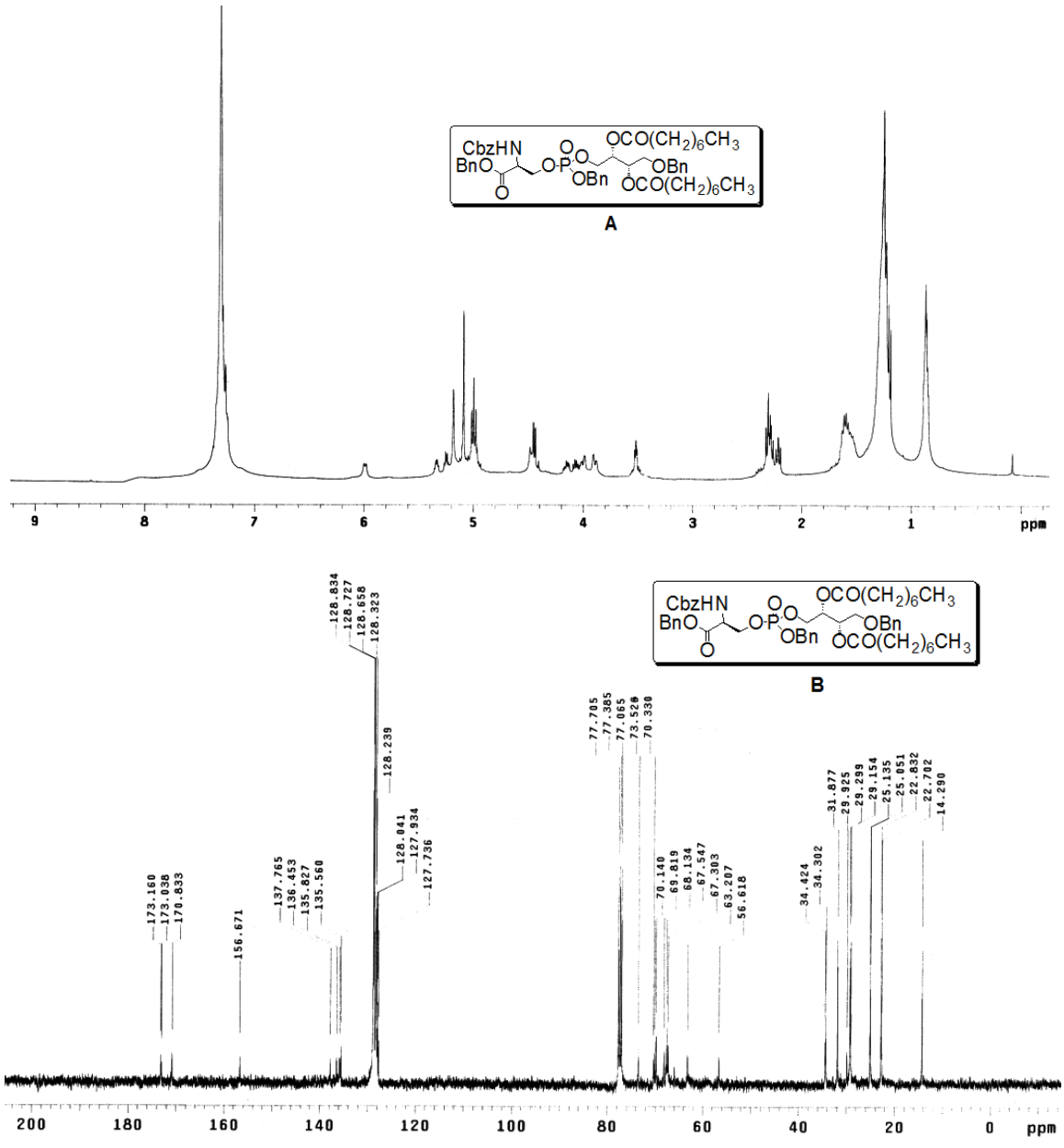

Figure S14. ^{1}H NMR (A) and ^{13}C NMR (B) spectra of compound **17**.

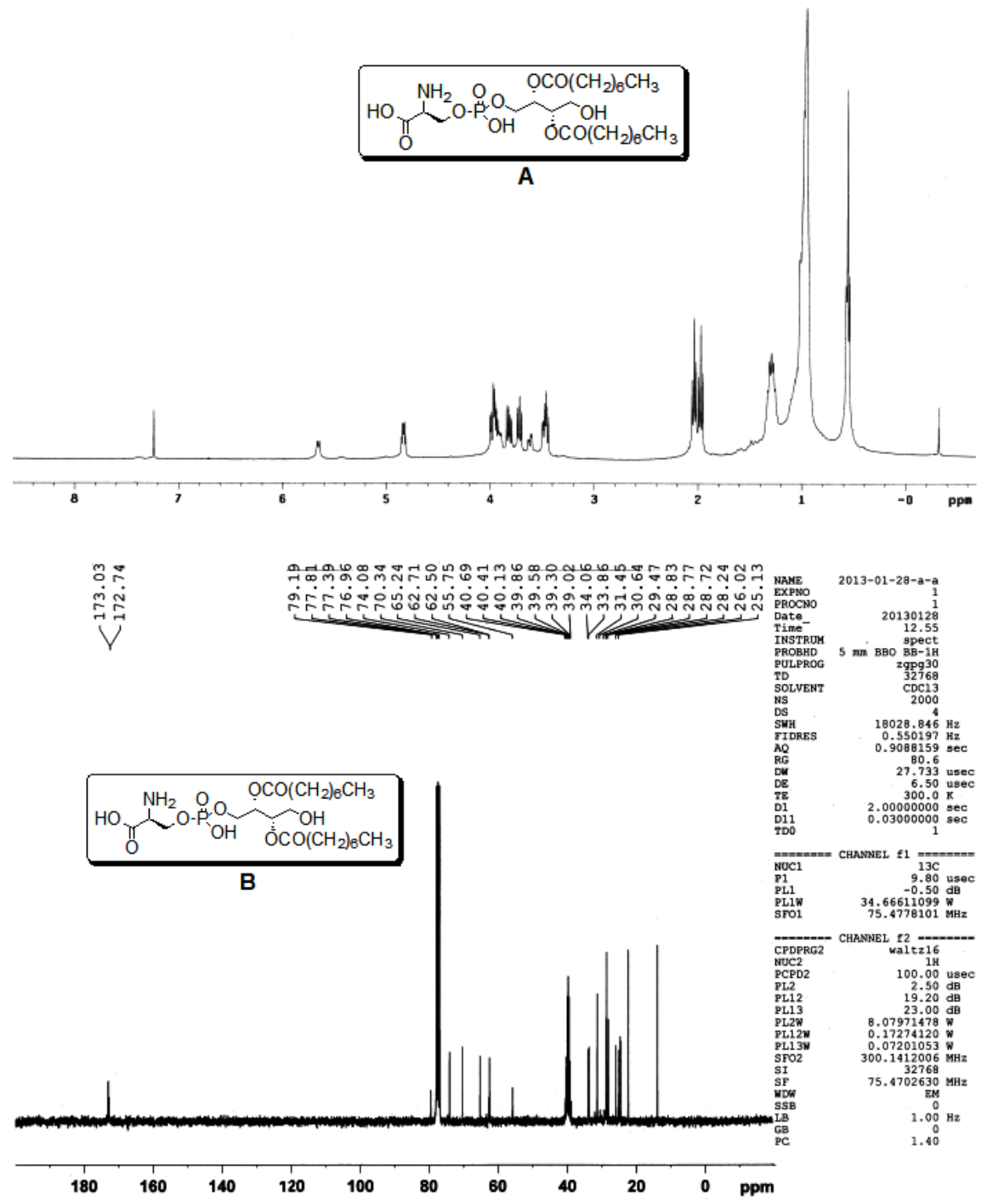

Figure S15. ^{1}H NMR (A) and ^{13}C NMR (B) spectra of DAT-PS$_8$.

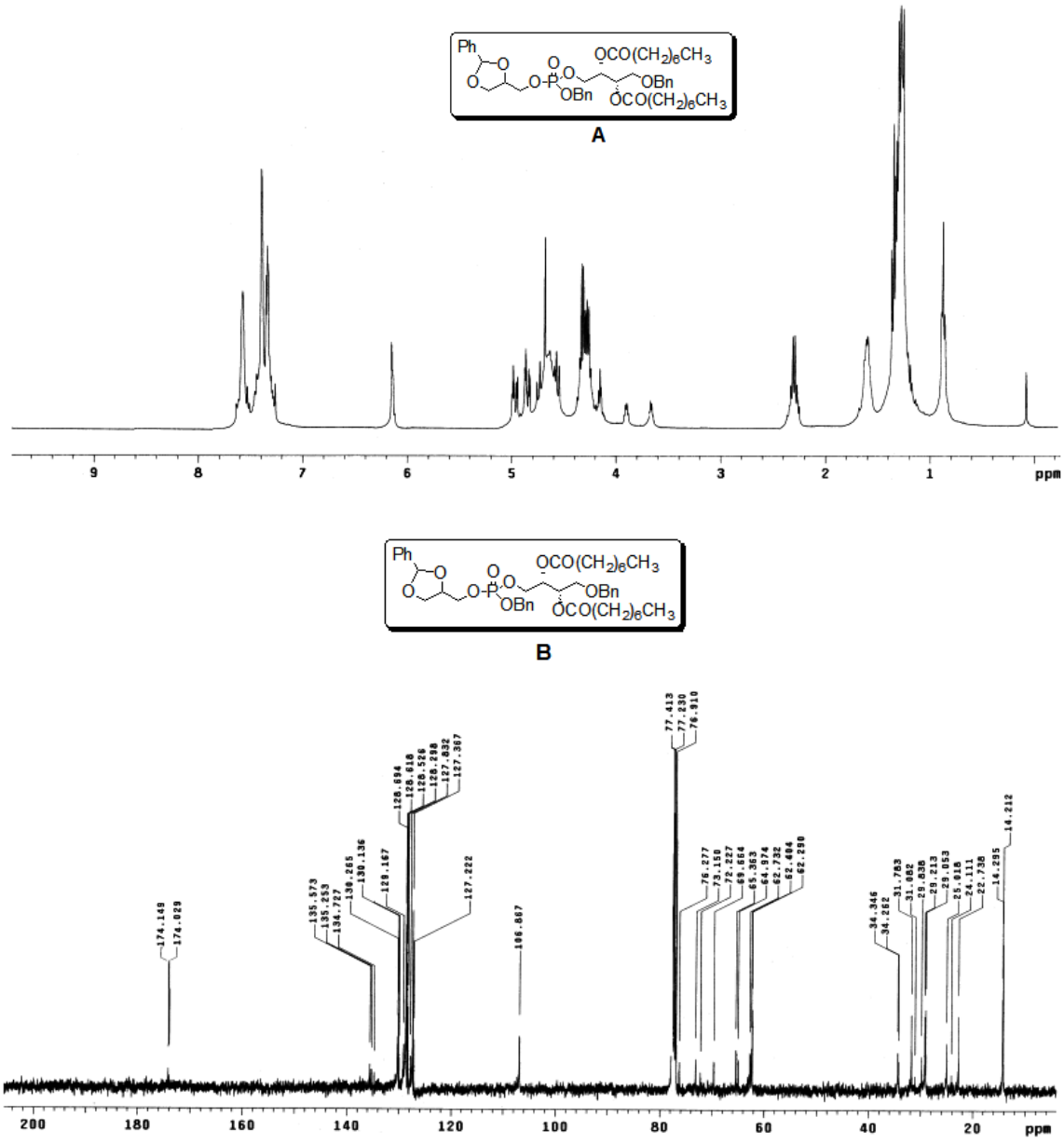

Figure S16. ^{1}H NMR (A) and ^{13}C NMR (B) spectra of compound **18**.

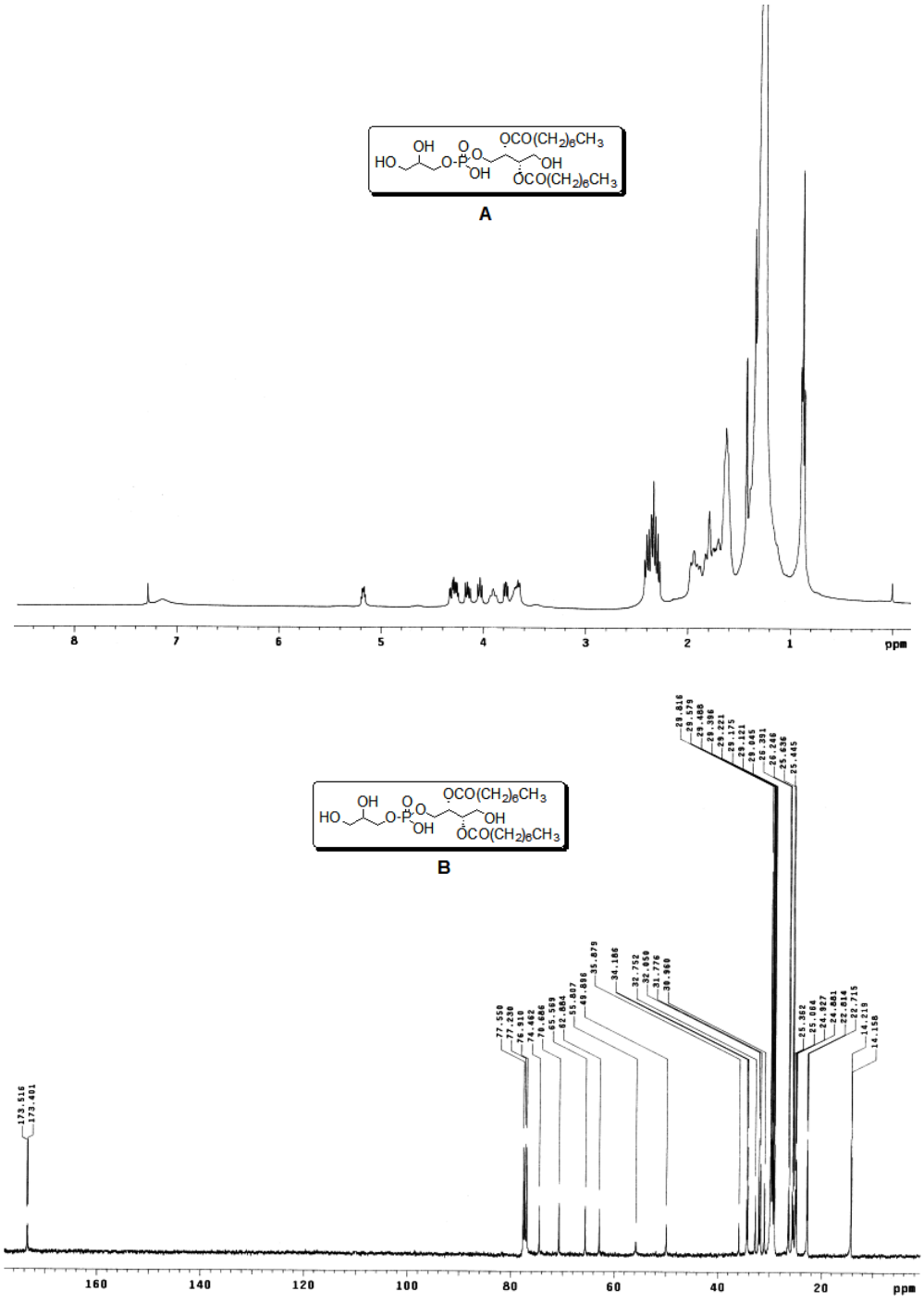

Figure S17. ^{1}H NMR (A) and ^{13}C NMR (B) spectra of DAT-PG_8.

^{31}P NMR Spectra of the New Compounds

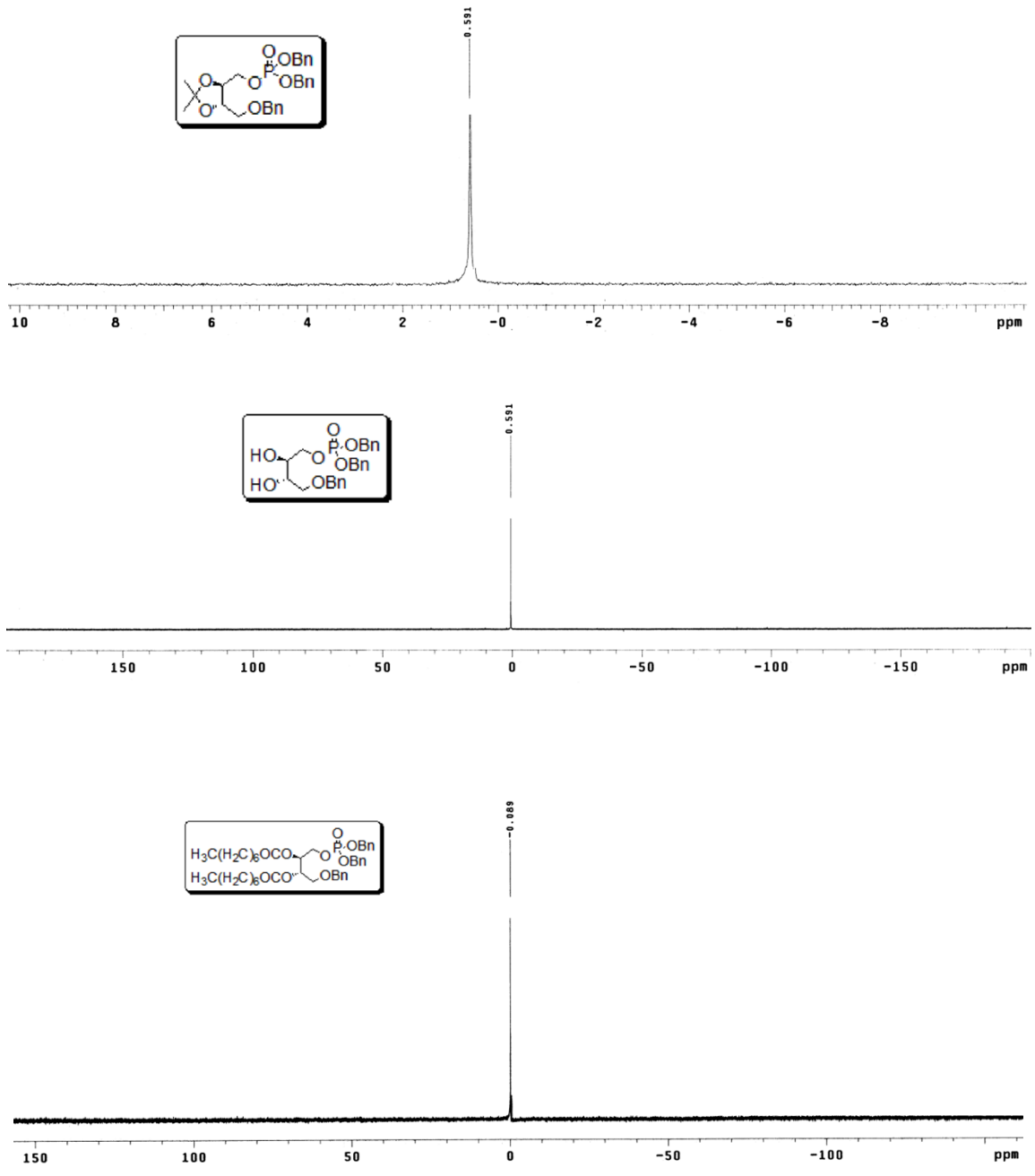

Figure S18. ^{31}P NMR spectra of compound **5**, **6**, and **7**.

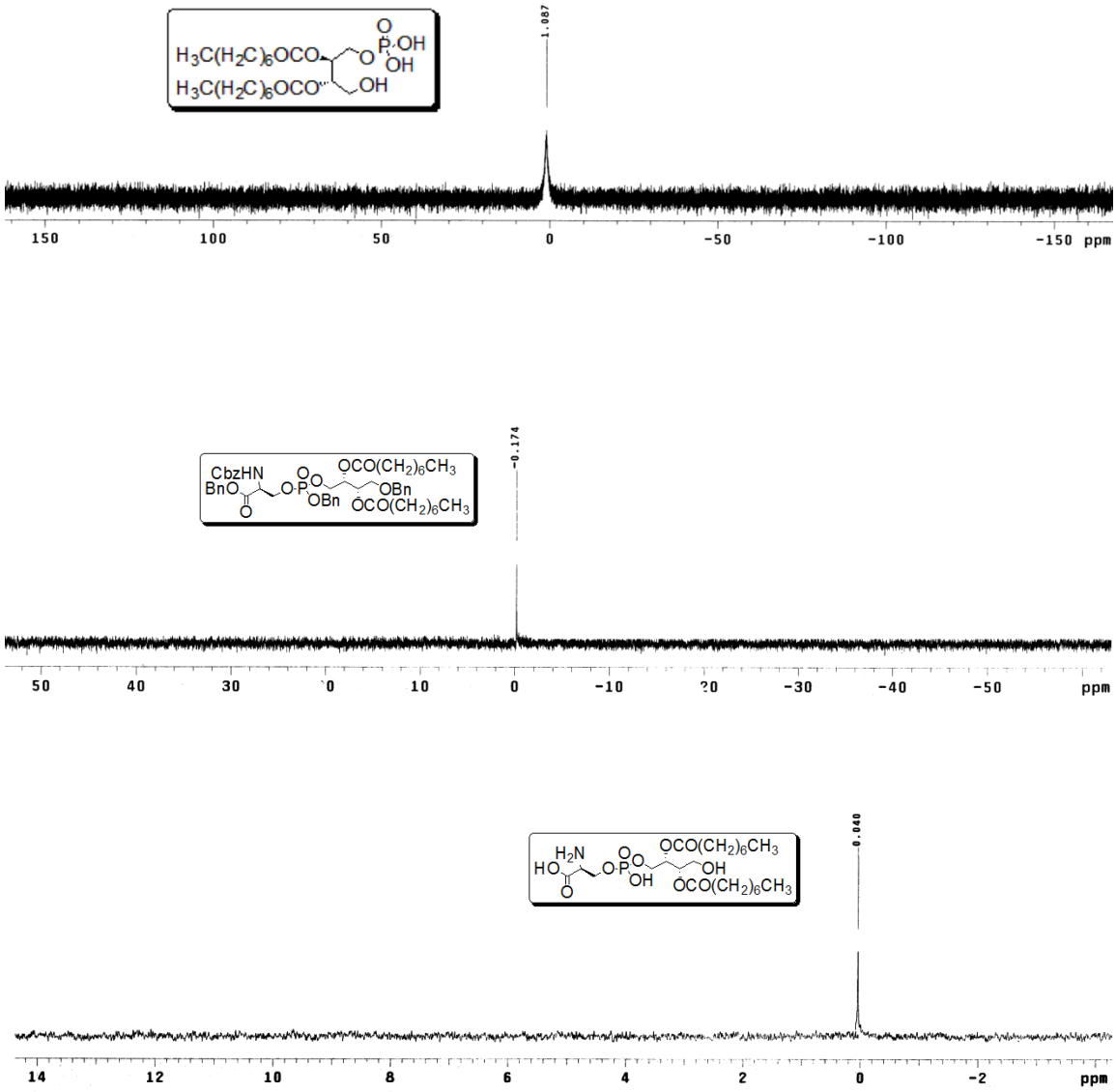

Figure S19. ^{31}P NMR spectra of compound DAT-PA$_8$, **17**, and DAT-PS$_8$.

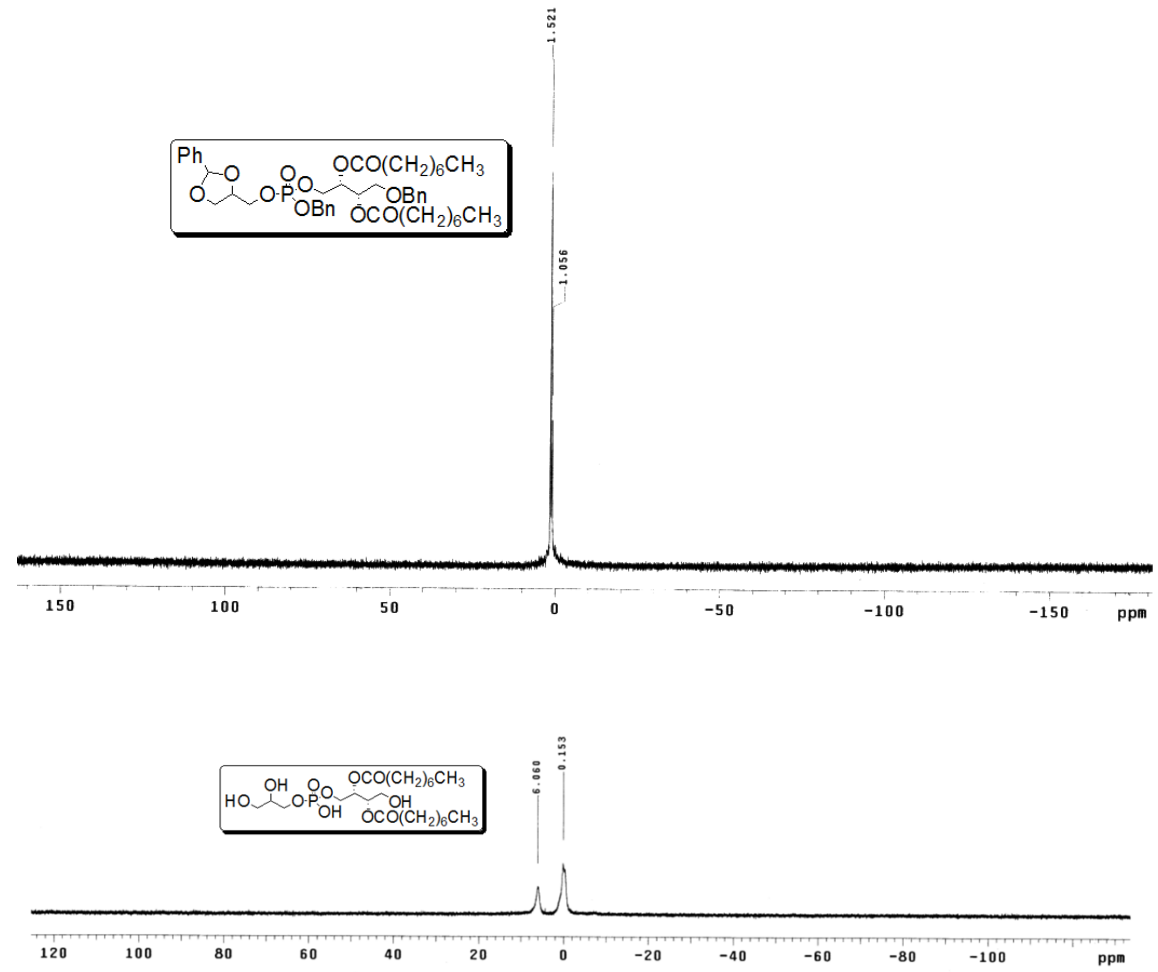

Figure S20. ^{31}P NMR spectra of compound **18** and DAT-PG$_8$.

HRMS Spectra of the New Compounds

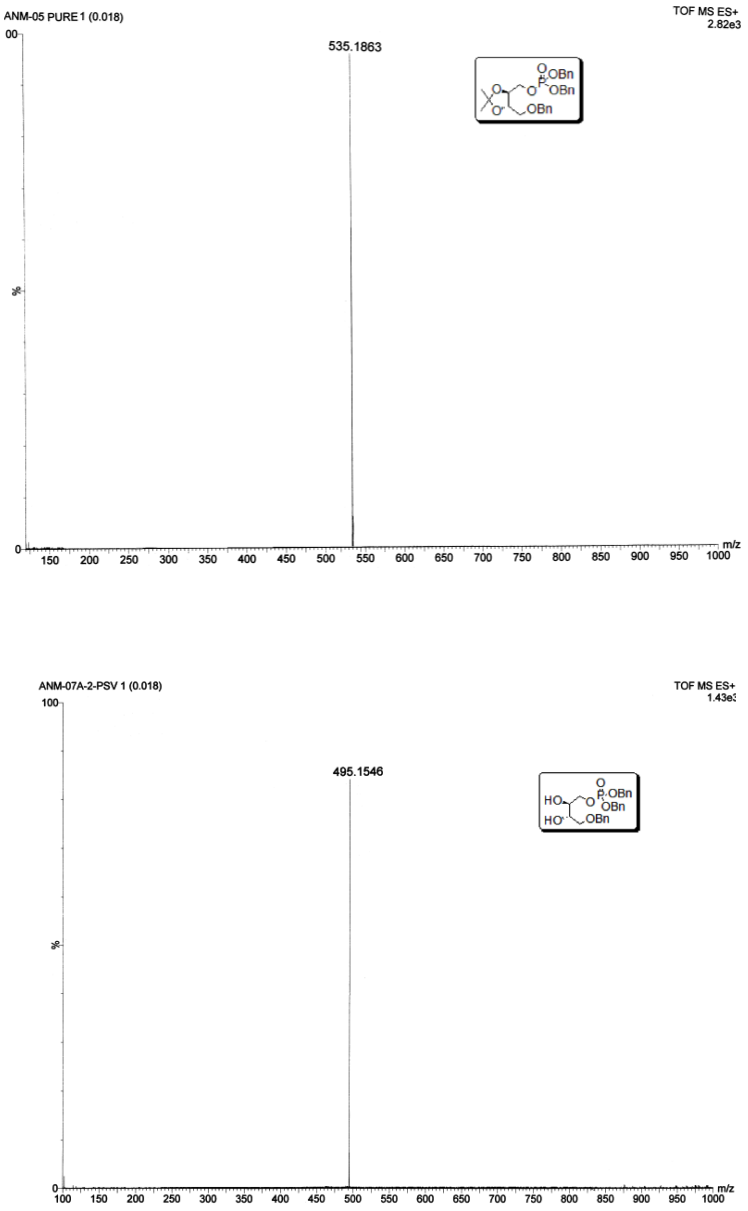

Figure S21. HRMS spectra of compound **5** and **6**.

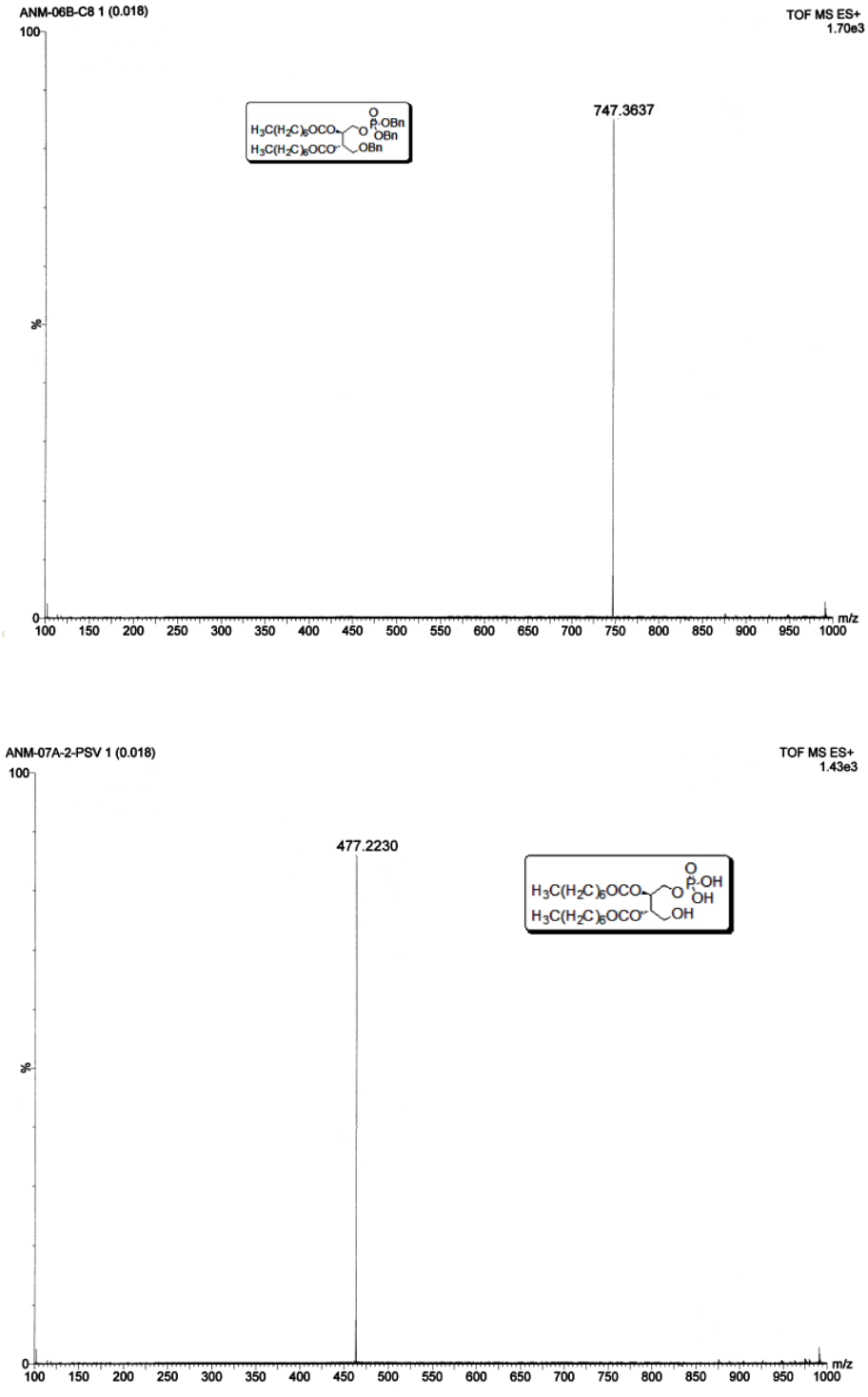

Figure S22. HRMS spectra of compound **7** and DAT-PA$_8$.

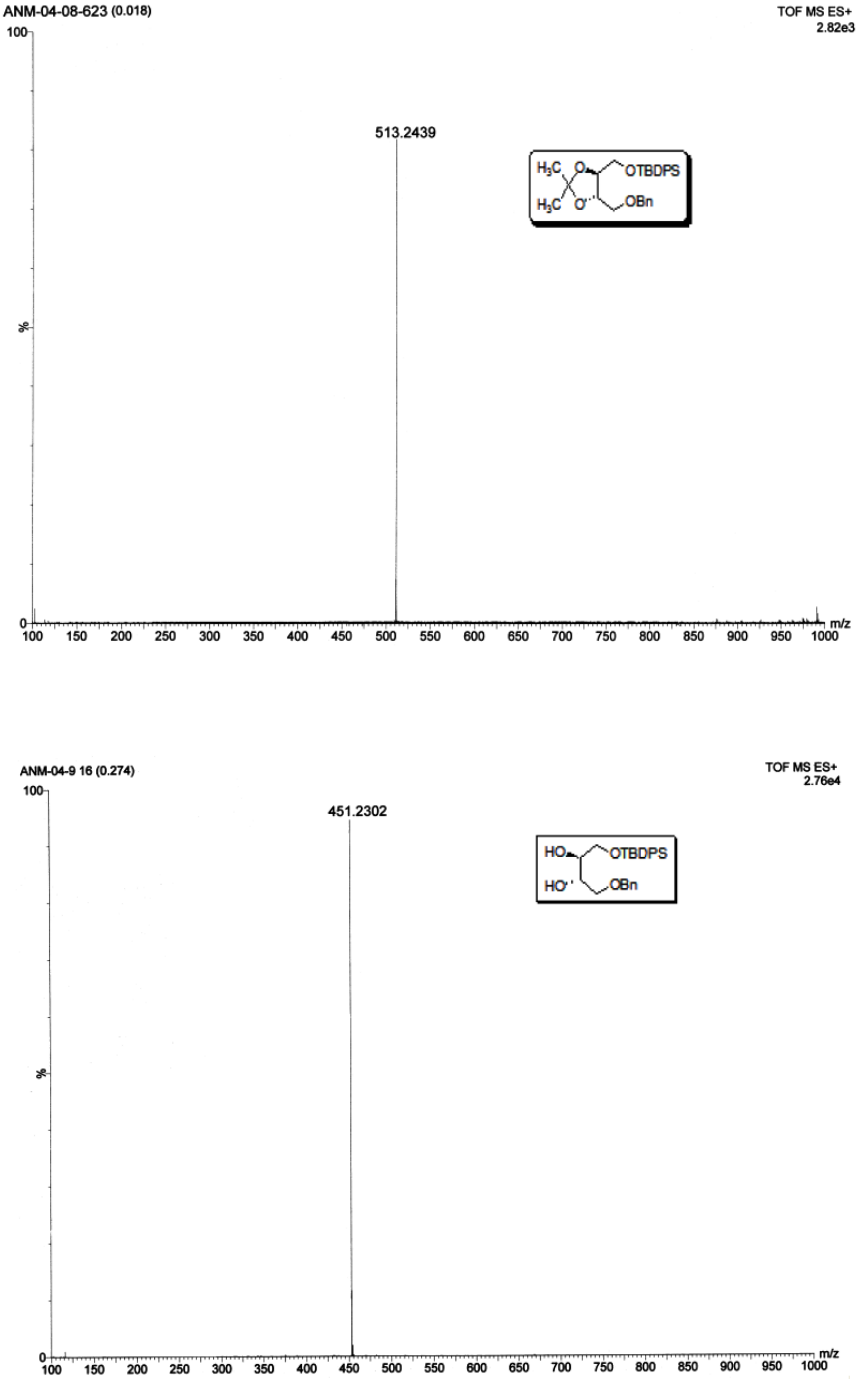

Figure S23. HRMS spectra of compound **13** and **14**.

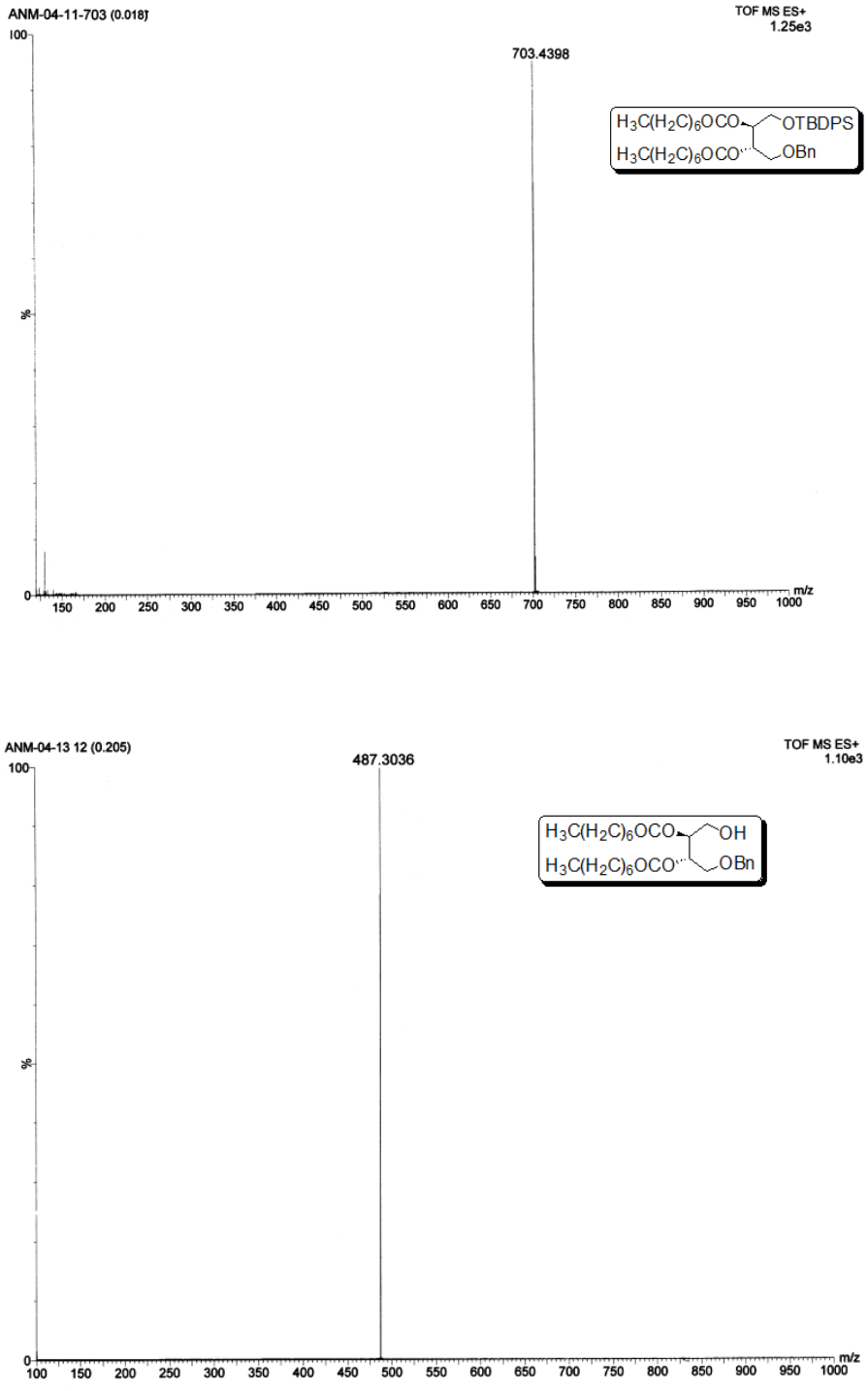

Figure S24. HRMS spectra of compound **15** and **16**.

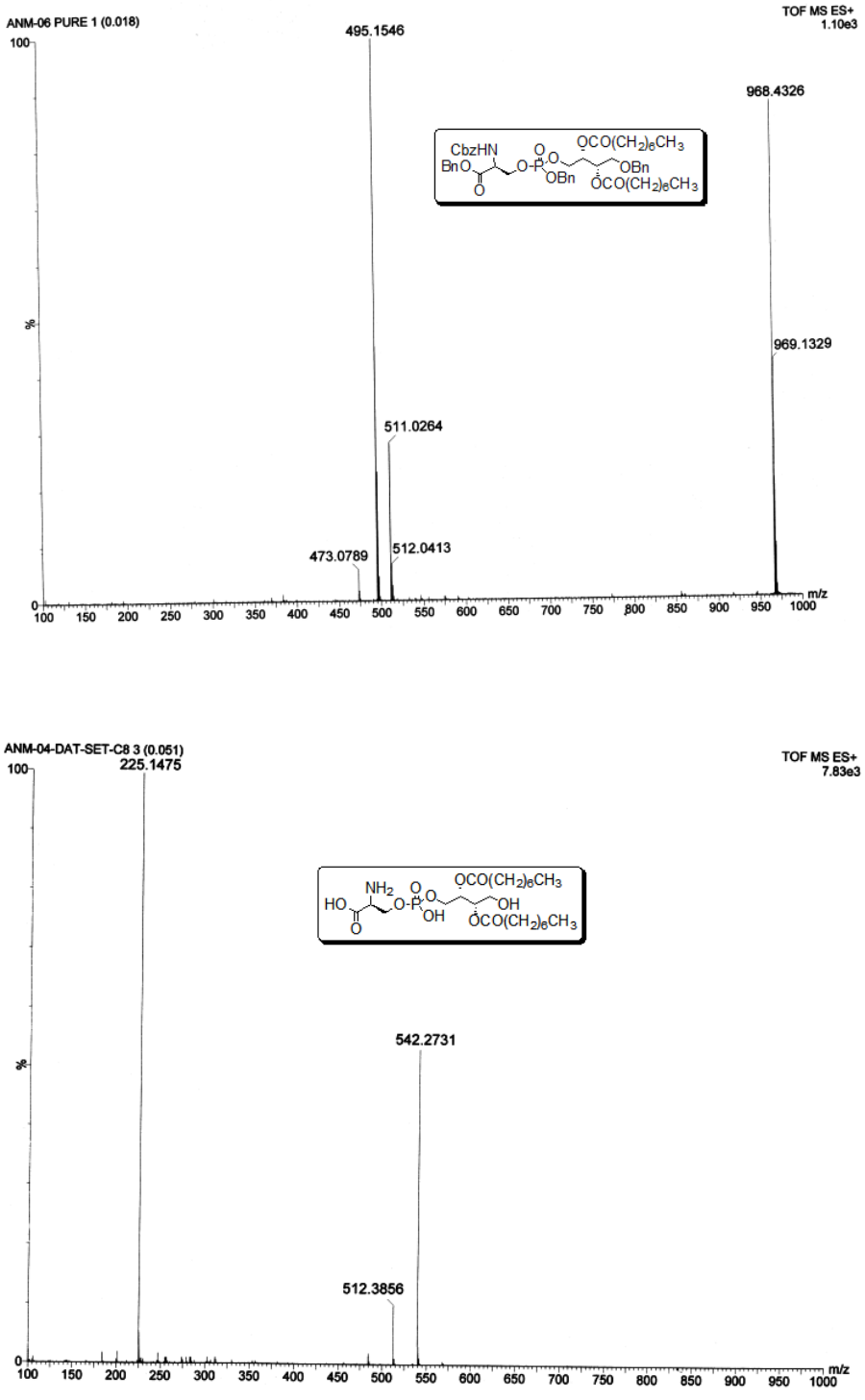

Figure S25. HRMS spectra of compound **17** and DAT-PS_8.

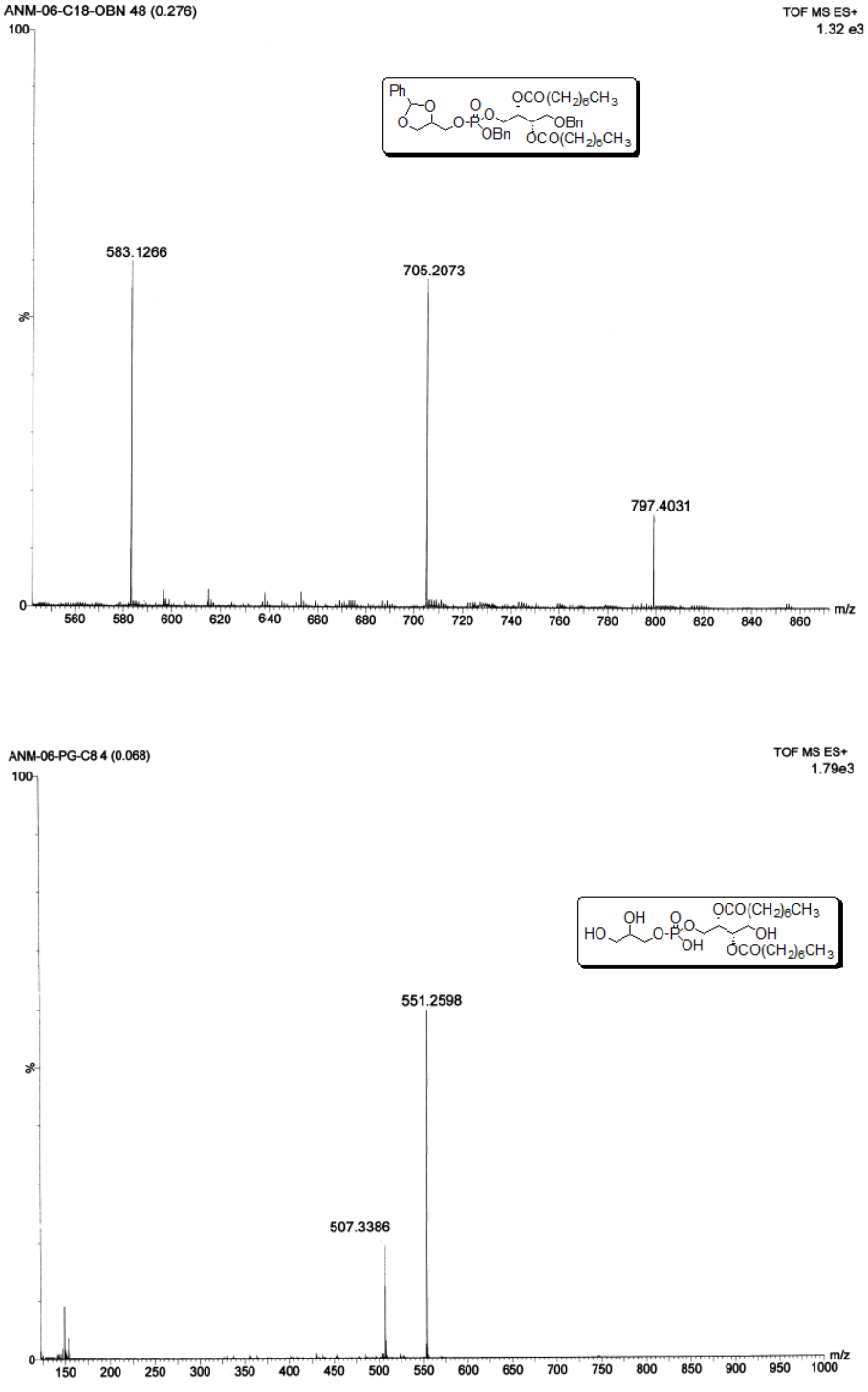

Figure S26. HRMS spectra of compound **18** and DAT-PG_8.